Multivariate ‘AND-gate’ substrate probes as enhanced contrast agents for fluorescence-guided surgery

John C. Widen[1], Martina Tholen[1], Joshua J. Yim[1,2], Kerriann M. Casey[4], Stephan Rogalla[5,6] & Matthew Bogyo[1,2,3]

[1]Department of Pathology, [2]Department of Chemical and Systems Biology, [3]Department of Microbiology and Immunology, [4]Department of Comparative Medicine, [5]Department of Pediatrics, and [6]Department of Radiology, Stanford University School of Medicine, Stanford, California, USA

The greatest challenges for surgical management of cancer are precisely locating lesions and clearly defining the margins between tumors and normal tissues. This is confounded by the characteristics of the tissue where the tumor is located as well as its propensity to form irregular boundaries with healthy tissues. To address these issues, molecularly targeted optical contrast agents have been developed to define margins in real time during surgery[1,2]. However, selectivity of a contrast agent is often limited by expression of a target enzyme or receptor in both tumor and healthy tissues. Here we introduce a concept of 'AND-gate' optical imaging probes that require sequential processing by multiple tumor-specific proteases to produce a fluorescent signal. This results in dramatically improved specificity as well as overall enhanced sensitivity. This general approach has the potential to be broadly applied to selectively target complex patterns of enzyme activities in diverse disease tissues for detection, treatment and therapy response monitoring.

For many cancers, surgery is the primary treatment option followed by chemo and/or radiation therapy. Early detection and surgical removal of solid tumors currently remain the most effective way to produce a curative result. Success outcomes are highly dependent on how effectively the tumor tissue can be identified[2,3]. Accurate detection of the 'margin' between tumor and normal healthy tissues is essential to prevent either incomplete removal of tumor cells leading to increased recurrence rates (up to 30-65% of cases)[4-6] or removal of excess healthy tissue. Furthermore, solid tumors derived from different tissues and cell types can have dramatically different margin borders, making the prospects for complete removal highly variable[7]. In fact, rates of repeat surgeries for some cancer types (i.e. breast) can be as high as 50%[3,8]. Therefore, new methods that allow both selective and sensitive real-time detection of tumor margins have the potential to have a significant impact on surgical treatment outcomes of many of the most common types of cancer.

Systemically delivered optical contrast agents have the potential to broadly highlight tumor sites without any prior knowledge of tumor location. Currently, there are only a few optical agents that are FDA approved for use in humans and that are suitable for use with clinical camera systems. While there has been significant clinical benefit from dyes such as ICG[9] and 5-ALA[10], the main limitation is their overall non-specific mechanism of action resulting in insufficient sensitivity and selectivity for use in diverse cancer types. A number of pre-clinical and early-stage clinical trials have begun for fluorescently tagged affinity agents such as antibodies, peptides and small molecule ligands[1,2,11]. There have also been significant advances in the development of "smart" probes that only produce a fluorescent signal when processed by a tumor-specific enzyme (**Fig. 1a**). This leads to a further increase in contrast because free probe outside the tumor remains unprocessed and is not fluorescent. Proteases have become the enzymes of choice for generation of smart probes because short peptide substrates can be decorated with suitable fluorophore/quencher pairs such that probes are optically silent until cleaved by a protease[12-15]. Protease activity can also be used to process probes that then change their localization to be retained in cells within the tumor microenvironment[14,16]. Multiple proteases have proven to be useful biomarkers of cancerous tissues[17-20].

Previously, we designed a cysteine cathepsin-cleavable NIR substrate probe 6QC-NIR[16]. Cleavage of this substrate probe produces high signals in cancers of the lung, breast, and colon, which can be detected with the FDA-approved da Vinci® Si Surgical System equipped with the Firefly® detection system[16,21]. However, cathepsins are active in both healthy tissues as well as inside the tumor microenvironment, which limits contrast in some locations. Here we describe a way to dramatically increase the overall tumor-selectivity by designing multivariate 'AND-gate' probes in which two reporters must be sequentially processed within the tumor microenvironment to produce a specific optical signal (**Fig. 1b, c**). Thus, selectivity can be

greatly enhanced because identification of the tumor tissue is made using multiple markers that help to distinguish it from the surrounding normal tissues.

The design of a general 'AND-gate' strategy involves placement of a fluorescent reporter in a central location such that multiple quenchers can be attached through linkages that are severed by the action of enzymes. This type of 'hub and spoke' model, requires removal of all quenchers along the spokes to liberate the central fluorescent hub. In theory, the quencher groups can be attached to the central hub using any type of enzyme-sensitive linkage resulting in AND-gates that are responsive to a diverse array of enzyme signatures. We choose to test this design strategy using a simple glutamic acid (Glu) central linker containing a fluorescent dye linked to quenchers through distinct peptide sequences that could be orthogonally cleaved by two proteases with non-overlapping substrate specificities. The central Glu linker is ideal because a sulfo-Cy5 fluorophore can be attached to its free amine and each peptide substrate containing a sulfo-QSY21 quencher can be connected through amide bonds to the remaining carboxylic acids (**Fig. 1d**). This positions the quenchers such that fluorescence activation occurs only after both peptides have been cleaved. Furthermore, by using simple diamino-alkyl linkers between the peptides and the Glu core, the final fluorescent fragment will contain two free amine groups that induce lysosomal accumulation of the probe, as we have demonstrated for our cathepsin substrate probes[16]. We chose peptide substrates that have already been shown to be specifically processed by caspase 3 (Casp3; DEVDGP)[22] and the cysteine cathepsins (Cats; Z-FK)[23]. These sequences are optimal for a first generation AND-gate probe because Casp3 and Cats have highly orthogonal substrate specificities and therefore each protease can only process its corresponding substrate. Furthermore, Cats are upregulated in both tumor associated macrophages (TAMs)[24-26] and in most normal tissues, while Casp3 activity is elevated in tumors but is generally not active in healthy cells, except during development[27].

Therefore, Cats and Casp3 are both active within tumors but are not expected to be active together in healthy tissues, making them ideal targets for our AND-gate probe strategy.

We synthesized a first-generation probe, **AND-Gate 1,** containing the natural (L)-Glu central linker (**Fig. 1d**, **Supplementary Scheme 1**). We also synthesized negative controls in which a (D)-Asp was used in place of the natural (L)-Asp in the P1 position of the Casp3 sequence (**(D)-Asp 1**) and a (D)-Phe was used in the P2 position of the Cat sequence (**(D)-Phe 1**). To test the **AND-Gate 1** probe, we incubated it with recombinant human CatL, B, S, or Casp3 either separately or sequentially in combinations (**Supplementary Fig. 1a,b**). Importantly, we found that the probe only produced a fluorescent signal when both cathepsin and casp3 were incubated sequentially. We also found that both control probes remained non-fluorescent after incubation with both proteases, regardless of order of addition, thus validating the overall concept of the AND-gate strategy (**Sup Fig. 1c,d**). We then tested the stability of the linker using total tissue lysates derived from homogenized 4T1 breast tumors (**Sup Fig. 1e**). We found that, as expected, the **AND-Gate 1** probe was activated and the **(D)-Asp 1** negative control remained non-fluorescent. However, the **(D)-Phe 1** probe showed robust activation, suggesting a lack of stability at the amide bond connection between the Z-FK substrate and the linker. Given the instability at the glutamine α-acid, we synthesized a 2nd generation probe **AND-Gate 2** and the respective negative controls **(D)-Phe 2** and **(D)-Asp 2**, in which the natural (L)-Glu was replaced by the unnatural (D)-Glu (**Fig. 2**). We evaluated this 2nd generation set of probes using the *in vitro* fluorogenic assay with recombinant proteases and found that the probes performed similarly to the first generation probes with only **AND-Gate 2** producing signal, and only after addition of both CatL and Casp3 (**Fig. 2a,b**). Importantly, the second-generation probes containing the D-Glu linker showed good stability in tumor lysates, with both negative probes remaining inactive even after 2 hours of incubation (**Fig. 2c**). The **AND-gate 2** was also selective for Casp3 over other related initiator and executioner caspases (**Sup Fig. 2**).

Having solved the issue of linker stability, we tested the specificity of activation of the **AND-Gate 2** probe using a co-culture of 4T1 cells and RAW macrophages. Cells were first incubated with DMSO or the cytotoxic agent etoposide (5 μM) for 24 h to induce apoptosis. The **6-QC**, **AND-Gate 2**, **Casp3-QC** (single substrate probe for Casp3, **Supplementary Figure 3**), and respective negative control probes were added to the cells for 2 h before acquiring images (**Fig. 2d**). As expected, **6-QC** was activated independently of apoptosis induction, while **AND-Gate 2** was activated only in the apoptotic cells (**Fig. 2e**).

We next evaluated the **AND-Gate 2** probe and its respective negative controls in a 4T1 mouse model of breast cancer. We imaged live animals 2 h post injection of probes and found that the **AND-Gate 2** probe showed strong tumor accumulation that resulted in a brighter tumor signal than the cathepsin only substrate **6-QC**, while the negative control probes produce no visible signals (**Fig. 3a**). Quantification of total tumor fluorescence confirmed that both the **AND-Gate 2** and single substrate probe **6-QC** produced a significantly increased signal compared to the negative controls **(D)-Phe 2** and **(D)-Asp 2**, and that this level of contrast over controls was several-fold higher for the AND-gate probe (**Fig. 3b**). The Casp3 specific substrate probe **Casp3-QC** showed a low-level tumor signal, however it was not significantly higher than the two negative control probes. The tumor-to-background ratio (TBR) for the **AND-Gate 2** was also significantly increased over the single-parameter **6-QC** probe (3.0 ± 0.3 compared to 2.3 ± 0.5; **Supplementary Fig. 4**). In order to determine the overall tumor selectivity of the probes, we excised relevant organs for *ex vivo* imaging and quantified the background corrected signals. Importantly, we found that the fluorescent signals in excised liver, kidneys, and lung tissue was significantly reduced in the animals treated with the **AND-Gate 2** compared to those treated with **6-QC** (**Fig. 3c**). Quantification of the fold change in fluorescent signals over tumor signals for each tissue confirmed the dramatic increase in selectivity of the AND-gate probe compared to the cathepsin-only **6-QC** probe (**Fig. 3d**). As a further analysis of probe activation *in vivo*, we

fixed and embedded excised tumors for cryo-sectioning and histological analysis using fluorescence microscopy (**Fig. 3e**). We stained tumor sections for CD68, a marker for macrophages, as well as for cleaved Casp3. This analysis confirmed the presences of macrophages within the 4T1 breast tumors, as has been previously described[16]. We also observed numerous regions within the tumor tissues where cells contained active Casp3. These regions of apoptotic cells were always found directly adjacent to, or co-localized with, macrophage cell populations. Furthermore, we observed the signal from the activated **AND-Gate 2** probe within the population of cells that were positive for CD68 and in close proximity to apoptotic cells. The brightest probe signal was always found at the intersection between macrophages and cells with active Casp3 confirming that Casp3 and Cats are both active within a tumor and generally found in close proximity making them ideal targets for use in the AND-gate strategy.

Next, we compared the performance of **AND-Gate 2** compared to the single substrate cathepsin probe **6-QC** in an $apc^{min/+}$ colorectal cancer mouse model. This model provides an opportunity to test the AND-Gate probe in a spontaneous cancer model containing a genetically distinct cancer from that of the 4T1 breast tumor model. Polyps in this model are difficult to distinguish from healthy tissue by eye due to their small size. Mice containing colonic polyps were injected with either probe and sacrificed 16 h post injection. Overall, both probes were able to fluorescently label polyps within the colons of mice after systemic injection (**Fig. 4**). Using the fluorescent signal from the probes, we chose areas of high, medium, and low fluorescent signal to be sectioned, stained for hematoxylin and eosin (H&E), and evaluated for the presence of tumor. Areas containing high or medium fluorescence intensity were expected to contain tumor while areas with low fluorescence intensity were expected to be healthy. The evaluated sections were determined to be true positive (TP), false positive (FP), true negative (TN), or false negative (FN) based on the expected and actual outcomes for the presence of tumor (**Fig. 4c**).

This analysis determined that the **AND-Gate 2** probe had a lower false positive rate (FPR) and false negative rate (FNR) compared to **6-QC** (0.25 vs 0.33 FPR and 0.19 vs 0.25 FNR). Based on this analysis, the two probes are comparable in their ability to highlight polyps in this colorectal cancer mouse model but the **AND-Gate 2** has a higher accuracy compared to the single substrate probe **6-QC**.

Overall, these studies provide a roadmap for the design of optical contrast agents that respond to unique enzymatic signatures that are indicative of a disease state. In the current design, we demonstrate the utility of the AND-gate approach using substrates that are uniquely processed by two proteases that are both activated in the tumor microenvironment. The design of the AND-gate protease probe used here required engineering of the linker group to prevent activation by undesired protease activities found in normal healthy tissues but ultimately resulted in a contrast agent that both improved tumor-selectivity and also increase tumor uptake resulting in a brighter overall signal. We are currently working to further optimize the central linker such that higher order probes can be rapidly generated by attachment of various substrates containing quenchers using orthogonal chemistry. This should allow synthesis of probes with high selectivity for diverse cancer types based on proteolytic signatures of those tumors. It also should, in principle, enable generation of probes that respond to other classes of enzymes that are capable of processing substrates to liberate a central fluorescent fragment.

METHODS

Chemistry Methods

See Supporting Information for synthetic protocols.

Biology Methods

General Cell Culture. 4T1 cells and RAW246.7 macrophages were cultured separately as previously describe[16,28]. RAW246.7 macrophages were cultured in Dulbecco's Modified Eagle's medium (DMEM) supplemented with 10% fetal bovine serum (FBS), and 100 units/ml penicillin and 100 µg/mL streptomycin. 4T1 cells were cultured in Roswell Park Memorial Institute (RPMI) 1640 medium with L-glutamine supplemented with 10% FBS, and 100 units/mL penicillin and 100 µg/mL streptomycin.

Fluorogenic Substrate Assay. All proteases were active site titrated as previously described to obtain active protease concentrations[16]. The buffers used for caspases and cathepsins were made as previously described[16,29]. The reducing agent 1,4-dithiothreitol (DTT) was freshly added to buffers just prior to use. All assays were conducted in black, opaque flat bottom 384-well plates (Greiner Bio-One). For single substrate probes and first cleavage of AND-Gate probes, compounds were diluted in the respective protease buffer from 10 mM stock solutions in DMSO, and 15 µL of substrate (20 µM) was added to each well. Immediately prior to beginning fluorescent measurements, 15 µL of protease was added to wells containing substrate using a multichannel pipette. All proteases were at a final concentration of 10 nM in the well unless otherwise indicated. Fluorescent measurements were read above the well with a Biotek Cytation3 Imaging Reader (7.00 mm read height, gain = 100, ex/em = 640/670, normal read speed).

After confirming AND-Gate probes are not activated upon single addition of protease, probes were incubated with single proteases in an Eppendorf tube prior to second protease addition and fluorescent measurements. AND-Gate probes or negative controls (40 µM) were initially digested in 20 nM protease in the respective protease buffer. After 2 h at 37 °C, reactions with cathepsin buffer (pH 5.5) were exhausted by addition of 2 M NaOH (1.4 µL/100 µL of buffer) and then diluted with caspase buffer to obtain a concentration of 20 µM total substrate (pH 7.0). Reactions containing caspase buffer (pH 7.0) was exhausted by addition of

1 M HCl (2 μL/100 μL of buffer) followed by dilution with cathepsin buffer to obtain a final concentration of 20 μM total substrate (pH 5.5). The singularly processed probes were added to wells (15 μL) and the second protease was added just prior to beginning fluorescent measurements (15 μL, 10 nM final protease concentration, 10 μM final substrate concentration). Fluorescent signal over time was measured as mentioned above.

Live Cell Fluorescent Microscopy Assay. RAW246.7 macrophages and 4T1 cells were diluted to 1 x 10^5 cells/mL with their respective media and then mixed in a 1:1 ratio. The mixture of cells were seeded in a 96-well, half-area, μclear® bottom, cell culture plate (Greiner Bio-One) at 30 μL per well, and allowed to adhere to the bottom of the plate for 24 h. Next, cells were incubated with DMSO (1 % v/v) or etoposide (5 μM). After 24h with DMSO or etoposide, probes were added to the cell media (5 μL, 1 μM) and incubated for 2 h. Then, Hoescht 33342 was added to the media (5 μg/mL) and the cells were imaged using a 40X oil emersion objective on a Zeiss Axiovert 200 M confocal microscope. Acquired Z-stacks consisted of 24 16-bit images taken in 1 μm increments apart beginning and ending 12 μm from the focal plane. The channels used were set on separate tracks. The channel settings were as follows: Cy5-Gain = 545, laser ex = 639 nm, 2% power, Hoescht 33342-gain = 750, laser ex = 405 nm, 4% power, and DIC-(T-PMT from Cy5 channel, gain = 480.

Images were processed using ImageJ. Images shown are flattened from Z-stacks by taking the maximum signal in each pixel. All images are adjusted to the same contrast and brightness levels. The corrected total cellular fluorescence (CTCF) was determined by manually tracing cells based on the DIC and nuclear staining images, and measuring the total fluorescence within each cell from the flattened Z-stack images. CTCF was calculated according to the following formula: CTCF = Integrated density – (area of cell x average background). The average background was obtained by tracing circles where no cells were present and averaging the overall signal. Cells that were overlapping or on the edge of the image were not counted.

For each condition, measurements are from n > 200 cells measured in at least six different wells from two biological replicates. CTCF measurements were normalized to **AND-Gate 2**, DMSO treated control to obtain fold-change values.

Animal Models and Fluorescent Imaging. All animal care and experimentation was conducted in accordance with current National Institutes of Health and Stanford University Institutional Animal Care and Use Committee guidelines. All *in vivo* and *ex vivo* imaging was conducted with a LiCor Pearl Trilogy imaging system using the 700 nm and white light image settings with a resolution of 170 µm. Live mice were imaged at indicated time points after R.O. or I.V. tail vein injection of probe under anesthesia (isofluorane). After imaging, mice were sacrificed under anesthesia by cervical dislocation.

4T1 Breast Tumor Model. 4T1 cells (ATCC) suspended in 1X PBS (100 µL, 1 x 10^6 cells/mL) were injected subcutaneously into the 3 and 8 mammary fat pads of 6-8 week old Balb/C ByJ female mice (Jackson Laboratory). Mice were monitored for tumor formation and were injected with probe for imaging between 7-10 days after seeding 4T1 cells. Probes were dissolved in 1X PBS (10% DMSO) and injected I.V. tail vein (100 µL, 20 nmol). Hair was removed to expose the tumors with Nair® lotion while the mice were under anesthesia 1 h prior to imaging. Mice per probe: n ≥ 5, three technical replicates where each probe was injected into at least one mouse for each replicate. Images were processed using LiCor Imaging Studio (Ver 5.2). Background corrected signal was obtained by drawing circles around tumors and then subtracting the signal directly adjacent to the tumor without hair. The areas of circles used to calculate the background corrected signal was the same for each tumor. Tumor-to-background (TBR) was calculated by placing two circles of the same size over the tumor and the exposed skin directly adjacent to the tumor and dividing the two fluorescent measurements.

Histological Analysis of 4T1 Tumor Sections using Confocal Fluorescence Microscopy. 4T1 breast tumors in the mammary fat pads of Balb/C mice injected with probe were excised post mortem. The tumor tissues were fixed in neutral buffered formalin solution (4% formaldehyde) for 24 h at 4 °C. The fixed tumor tissues were then soaked in 30% w/v sucrose in 1X PBS for 24 h at 4 °C. Tumor samples were embedded in Optimal Cutting Temperature (O.C.T.) compound and kept at -80 °C until further use. Embedded tissues were then crysosectioned (5 μm) onto glass slides. The samples were stored at -20 °C prior to staining. The cryosections were first washed with 1X PBS 3X in a slide chamber. Then, the samples were blocked with 3% w/v BSA for 24 h at 4 °C. Samples were washed 3X with 0.5% w/v BSA, then tissues were outlined with a hydrophobic pen, followed by incubation with 1:2,500 dilution of primary antibodies for CD68 (rat anti-mouse, ABD SeroTec) and cleaved Casp3 (rabbit anti-mouse, Cell Signaling) in 0.5% w/v BSA in 1X PBS for 24 h at 4 °C. Samples were then washed 5X with 0.5% w/v BSA in 1X PBS. Tissues were then incubated with anti-rat alexafluor488 and anti-rabbit alexafluor594 secondary antibodies (Invitrogen) diluted 1:5,000 for 1 h at RT. Tissues were washed 5X with 0.5% w/v BSA in 1X PBS, followed by 3X washes with 1X PBS. Tissues were mounted with Vectashield mounting medium containing DAPI.

Sections of tumors were imaged using a 40X oil emersion objective on a Zeiss Axiovert 200 M confocal microscope. Images are of a single focal plane (16-bit). All channels were set on separate tracks for imaging. The channel settings were as follows: Cy5–Gain = 730, laser ex = 639 nm, 20% power; A594(cleaved Casp3)–gain = 600, laser ex = 555 nm, 4% power; A488(CD68)–gain = 640, laser ex = 488, 4% power; DAPI–gain = 600, laser ex = 405 nm, 2% power.

$Apc^{min/+}$ Colorectal Cancer Model. $APC^{min/+}$ on the C57BL/6 background were purchased from Jackson Laboratories and maintained in a specific pathogen-free facility. Mice were allowed to age to 22 weeks to allow for polyps to develop before the experiment. Mice were injected with **6-**

QC or **AND-Gate 2** (R.O., 20 nmol, 100 µL) in 1X PBS containing 10 v/v % DMSO. Mice were euthanized 16 h post injection. Following euthanasia, colonic tissues were excised from the level of the cecum to the anus. The proximal, middle, and distal colon was linearized parallel to its longitudinal axis for visualization of mucosal polyps and placed on an index card (serosal surface down) to retain linear orientation. Brightfield and fluorescent imaging was performed as described above using a LiCor Pearl Imaging system. Following imaging, tissues were immersion fixed in 10% neutral buffered formalin for 72 hours and transferred to 70% ethanol.

Histopathological Analysis of $Apc^{min/+}$ mouse colons. Colonic tissues were grossly compared to fluorescent images for identification of targeted lesions. Areas of high, medium, and low fluorescent signal were chosen for sectioning and analysis. It was expected that areas containing high and medium fluorescent signal intensity would be positive for tumor tissue and areas of low signal would be healthy tissue. In total, n=50 distinct locations were selected (n=25 sections per probe) for histopathologic evaluation based on fluorescent signaling. Tissue sections were cut perpendicular to the longitudinal axis of the colon, processed routinely, embedded in paraffin, sectioned at 5 µm, and stained with hematoxylin and eosin (H&E). All sections were blindly evaluated by a board-certified veterinary pathologist for the presence or absence of mucosal polyps. If histopathologic results deviated from expected results based on fluorescent imaging (n=10), paraffin blocks were melted, rotated 90°, re-imbedded, and H&E stained to evaluate for polyps in various planes of section.

ACKNOWLEDGEMENTS

This work was supported by NIH grants R01 EB026285 (to M.B.), American Cancer Society Postdoc Fellowship (To J.W.), DFG Research Fellowship TH2139/1-1 (to M.T.), and Stanford ChEM-H Chemistry/Biology Interface Predoctoral Training Program and NSF Graduate

Research Fellowship Grant DGE-114747 (to J.J.Y). Special thanks to Scott Snipas in the Guy Salvesen Lab at Sanford Burnham Prebys Medical Discovery Institute for gifting the recombinant caspases used in this study. Thanks to the Turk Lab at J. Stefan Institute for providing the recombinant cathepsin proteases used in this study.

AUTHOR CONTRIBUTIONS

M.B. and J.C.W conceived of the AND-Gate probe concept and designed all experiments. J.C.W synthesized all AND-Gate probes, conducted the fluorogenic substrate assays, live and fixed cell fluorescent microscopy experiments, and mouse model experiments. J.C.W and M.B. wrote the text of the paper and constructed the figures with input from J.J.Y. M.T. and J.J.Y helped perform live and *ex vivo* imaging during the 4T1 cancer mouse model experiment including dissection of the mice. M.T. aided in the immunohistochemical analysis of 4T1 tumors. S.R. assisted in the colorectal cancer mouse model. K.C. conducted the sectioning, H&E staining, and analysis of sections for the colorectal cancer mouse model.

COMPETING FINANCIAL INTERESTS

The authors declare no competing financial interests.

REFERENCES

1. Garland, M., Yim, J.J. & Bogyo, M. A Bright Future for Precision Medicine: Advances in Fluorescent Chemical Probe Design and Their Clinical Application. *Cell Chem Biol* **23**, 122-136 (2016).

2. Tringale, K.R., Pang, J. & Nguyen, Q.T. Image-guided surgery in cancer: A strategy to reduce incidence of positive surgical margins. *Wiley Interdiscip Rev Syst Biol Med* **10**, e1412 (2018).

3. Orosco, R.K. et al. Positive Surgical Margins in the 10 Most Common Solid Cancers. *Sci Rep* **8**, 5686 (2018).

4. Yossepowitch, O. et al. Positive surgical margins after radical prostatectomy: a systematic review and contemporary update. *Eur Urol* **65**, 303-313 (2014).

5. Winter, J.M. et al. 1423 pancreaticoduodenectomies for pancreatic cancer: A single-institution experience. *J Gastrointest Surg* **10**, 1199-1210; discussion 1210-1191 (2006).

6. McGirt, M.J. et al. Extent of surgical resection is independently associated with survival in patients with hemispheric infiltrating low-grade gliomas. *Neurosurgery* **63**, 700-707; author reply 707-708 (2008).

7. Brouwer de Koning, S.G., Vrancken Peeters, M., Jozwiak, K., Bhairosing, P.A. & Ruers, T.J.M. Tumor Resection Margin Definitions in Breast-Conserving Surgery: Systematic Review and Meta-analysis of the Current Literature. *Clin Breast Cancer* (2018).

8. Morrow, M. et al. Trends in Reoperation After Initial Lumpectomy for Breast Cancer: Addressing Overtreatment in Surgical Management. *JAMA Oncol* (2017).

9. Gossedge, G., Vallance, A. & Jayne, D. Diverse applications for near infra-red intraoperative imaging. *Colorectal Dis* **17 Suppl 3**, 7-11 (2015).

10. Ferraro, N. et al. The role of 5-aminolevulinic acid in brain tumor surgery: a systematic review. *Neurosurg Rev* **39**, 545-555 (2016).

11. Nguyen, Q.T. & Tsien, R.Y. Fluorescence-guided surgery with live molecular navigation--a new cutting edge. *Nat Rev Cancer* **13**, 653-662 (2013).

12. Weissleder, R., Tung, C.H., Mahmood, U. & Bogdanov, A., Jr. In vivo imaging of tumors with protease-activated near-infrared fluorescent probes. *Nat Biotechnol* **17**, 375-378 (1999).

13. Whitley, M.J. et al. A mouse-human phase 1 co-clinical trial of a protease-activated fluorescent probe for imaging cancer. *Sci Transl Med* **8**, 320ra324 (2016).

14. Whitney, M. et al. Ratiometric activatable cell-penetrating peptides provide rapid in vivo readout of thrombin activation. *Angew Chem Int Ed Engl* **52**, 325-330 (2013).

15. Sakabe, M. et al. Rational design of highly sensitive fluorescence probes for protease and glycosidase based on precisely controlled spirocyclization. *J Am Chem Soc* **135**, 409-414 (2013).

16. Ofori, L.O. et al. Design of Protease Activated Optical Contrast Agents That Exploit a Latent Lysosomotropic Effect for Use in Fluorescence-Guided Surgery. *ACS Chem Biol* **10**, 1977-1988 (2015).

17. Egeblad, M. & Werb, Z. New functions for the matrix metalloproteinases in cancer progression. *Nat Rev Cancer* **2**, 161-174 (2002).

18. Parks, W.C., Wilson, C.L. & Lopez-Boado, Y.S. Matrix metalloproteinases as modulators of inflammation and innate immunity. *Nat Rev Immunol* **4**, 617-629 (2004).

19. Mohamed, M.M. & Sloane, B.F. Cysteine cathepsins: multifunctional enzymes in cancer. *Nat Rev Cancer* **6**, 764-775 (2006).

20. Aggarwal, N. & Sloane, B.F. Cathepsin B: multiple roles in cancer. *Proteomics Clin Appl* **8**, 427-437 (2014).

21. Yim, J.J., Tholen, M., Klaassen, A., Sorger, J. & Bogyo, M. Optimization of a Protease Activated Probe for Optical Surgical Navigation. *Mol Pharm* **15**, 750-758 (2018).

22. Stennicke, H.R., Renatus, M., Meldal, M. & Salvesen, G.S. Internally quenched fluorescent peptide substrates disclose the subsite preferences of human caspases 1, 3, 6, 7 and 8. *Biochem J* **350 Pt 2**, 563-568 (2000).

23. Blum, G. et al. Dynamic imaging of protease activity with fluorescently quenched activity-based probes. *Nature chemical biology* **1**, 203-209 (2005).

24. Gajewski, T.F., Schreiber, H. & Fu, Y.X. Innate and adaptive immune cells in the tumor microenvironment. *Nature immunology* **14**, 1014-1022 (2013).

25. Loser, R. & Pietzsch, J. Cysteine cathepsins: their role in tumor progression and recent trends in the development of imaging probes. *Frontiers in chemistry* **3**, 37 (2015).

26. Olson, O.C. & Joyce, J.A. Cysteine cathepsin proteases: regulators of cancer progression and therapeutic response. *Nature reviews. Cancer* **15**, 712-729 (2015).

27. Nikoletopoulou, V., Markaki, M., Palikaras, K. & Tavernarakis, N. Crosstalk between apoptosis, necrosis and autophagy. *Biochimica et biophysica acta* **1833**, 3448-3459 (2013).

28. Verdoes, M. et al. Improved quenched fluorescent probe for imaging of cysteine cathepsin activity. *Journal of the American Chemical Society* **135**, 14726-14730 (2013).

29. Edgington-Mitchell, L.E. & Bogyo, M. Detection of Active Caspases During Apoptosis Using Fluorescent Activity-Based Probes. *Methods Mol Biol* **1419**, 27-39 (2016).

Figures

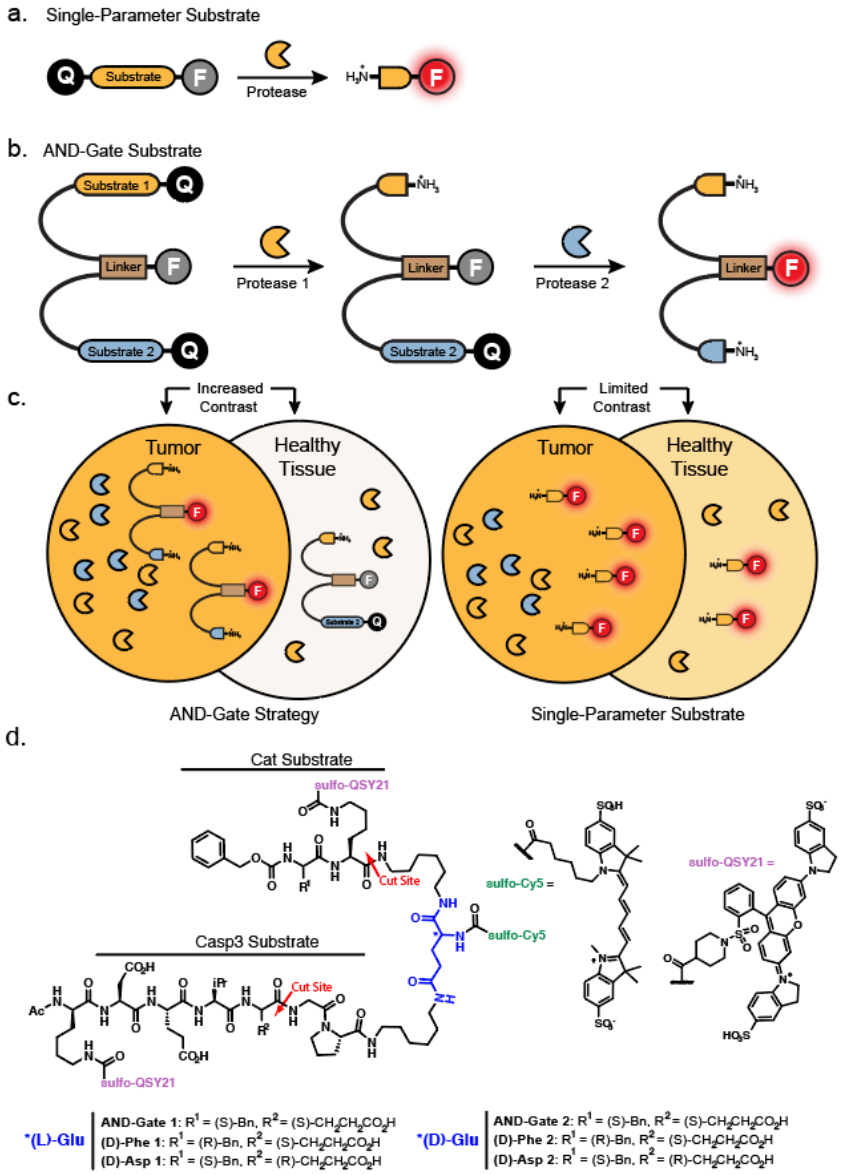

Figure 1 The AND-Gate strategy. (**a**) Schematic of a single-parameter quenched-fluorescent protease substrate that is cleaved by a single protease to produce a fluorescent fragment. These probes take advantage of higher proteolytic activity in tumors to generate contrast. (**b**) Schematic of the multivariate AND-Gate probe, which requires two proteolytic processing events to activate fluorescence. (**c**) Comparison of the single-parameter and AND-Gate probes in tumor and normal tissues. Higher contrast is generated by the AND-gate probe due to lack of activation in normal tissues which lack both protease activities. (d) Structures of the dual orthogonal protease substrate AND-Gate probes and negative controls. **AND-Gate 1** contains the natural amino acid (L)-Glu while the **AND-Gate 2** contains a non-natural (D)-Glu linker (blue). The negative control probes contain either a (D)-Asp in the P1 position of the Casp3 sequence (**(D)-Asp**) or (D)-Phe in the P2 position of the Cat sequence (**(D)-Phe**) to block proteolytic cleavage by the respective protease. Synthetic details for each AND-Gate probe can be found in the Supplementary Information.

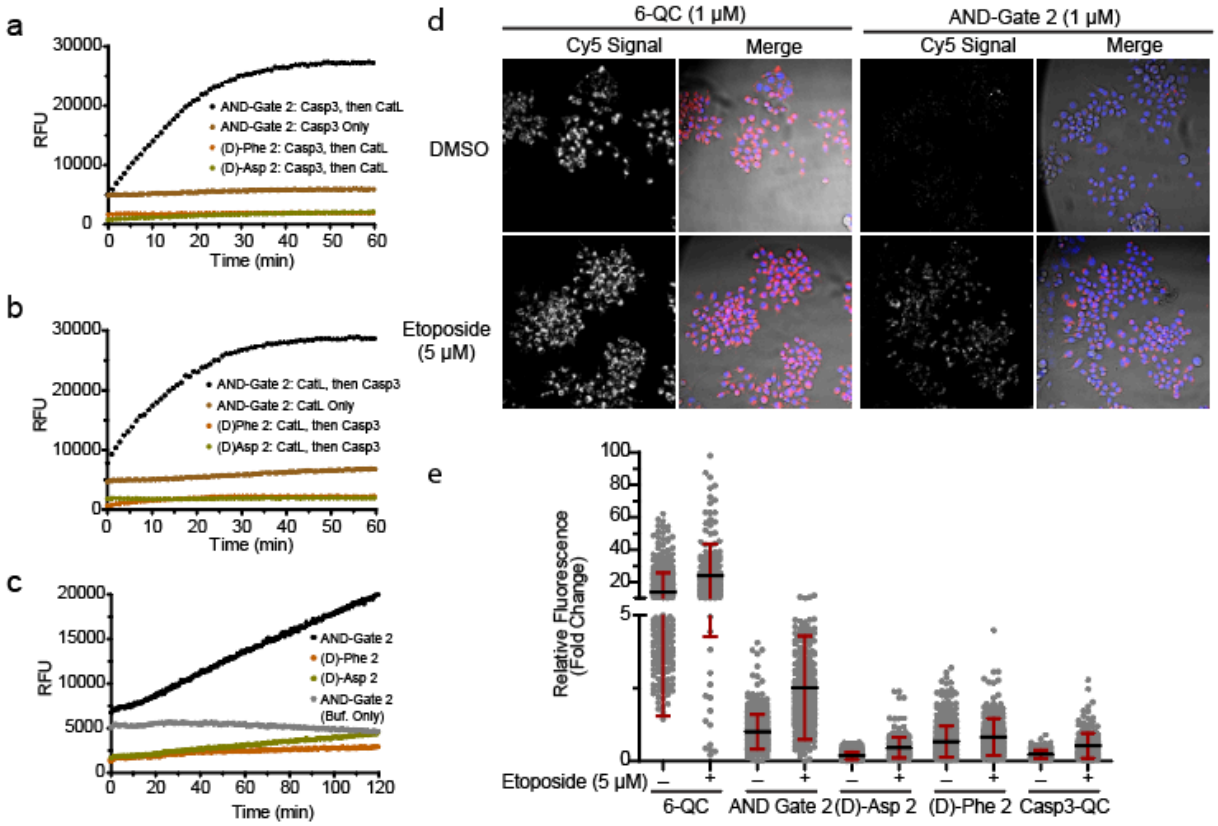

Figure 2 In vitro validation of the AND-gate strategy. (**a**) Progress curve of **AND-Gate 2** and negative control probes **(D)-Phe-2** and **(D)-Asp-2** after incubation with Casp3 (10 nM) alone or with Casp3 and then CatL (10 nM). All substrates were used at 10 μM. (**b**) Progress curves as in (**a**) except CatL was added first followed by cas3 (**c**) Progress curve over 2 hours incubation of the **AND-Gate 2** probe and corresponding negative controls, **(D)-Phe-2** and **(D)-Asp-2**, in either buffer or tumor lysate generated from 4T1 breast tumors in female Balb/C mice. (**d**) Representative fluorescent microscopy images of 4T1 cells co-cultured with RAW macrophages (1:1 ratio) labeled with either the single-parameter cathepsin probe **6-QC** or the **AND-gate 2** probe. Cells were incubated with either DMSO or etoposide (5 μM) for 24 h prior to addition of probes (1 μM). After 2 h, Hoechst stain was added to visualize nuclei and the cells were imaged. The Cy5 signal is shown in gray scale in the left panels and for the merged images on the right the brightfield is in grayscale. Blue is nuclear staining and red is the Cy5 probe signal. (**e**) Scatter plot of fluorescent signal from (**d**) shown as the fold change of corrected total cellular fluorescence normalized to cells incubated with DMSO and **AND-Gate 2**.

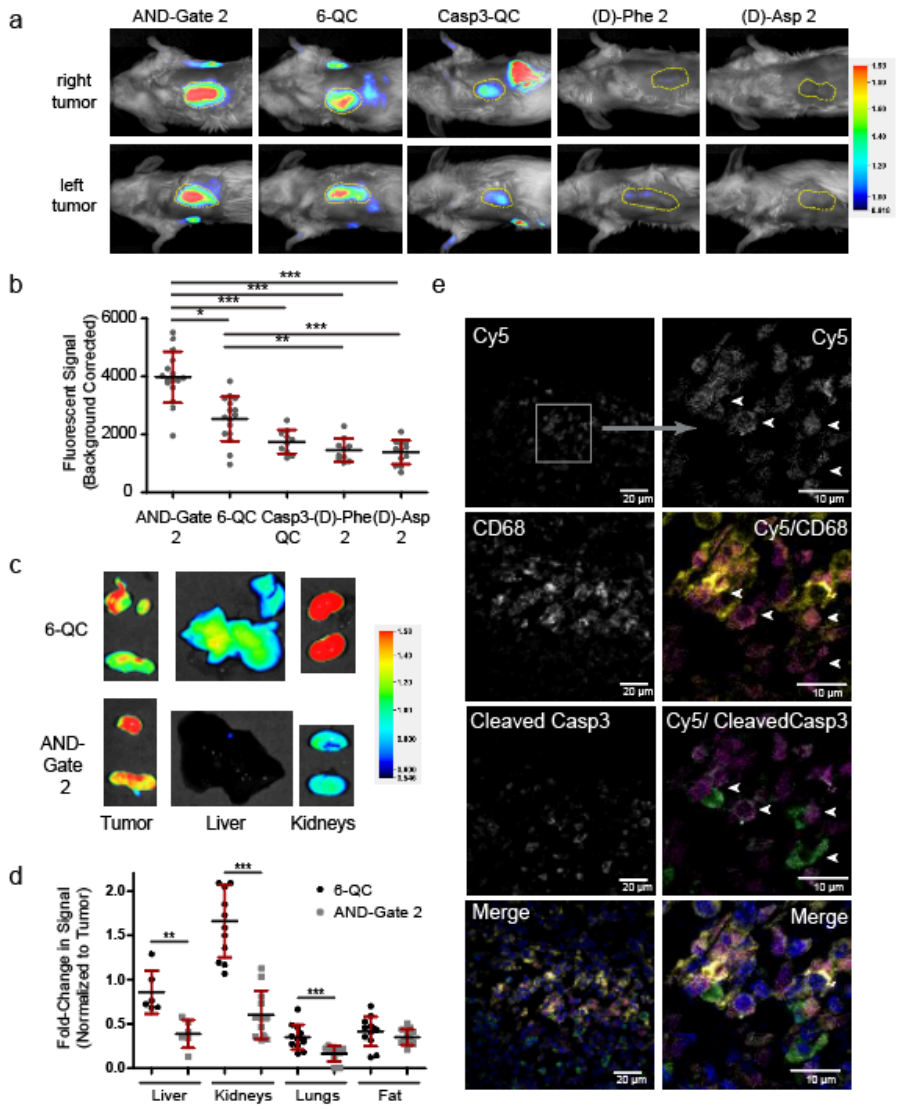

Figure 3 Enhanced selectivity and sensitivity of the AND-gate probe. (**a**) Images of balb/C mice bearing 4T1 breast tumors 2 hr after probe injection (20 nmol). Fluorescent signal in tumors is displayed as rainbow plots and is normalized across representative images from each cohort. Tumor outlines are indicated with yellow dotted lines. Images of all mice can be found in the extended data. (**b**) Scatter plot of average background corrected signal from all mice injected with each probe. (Tukey's Test: *$p < 0.05$, **$p < 0.01$, ***$p < 0.001$). (**c**) Images of excised organs of mice after *in vivo* imaging (2 h post injection). Fluorescent signal is displayed as rainbow plots and is normalized between images. Images are representative of each cohort. Images for all excised tumors and healthy tissues from each cohort can be found in the Supplementary Information. (**d**) Scatter plot of the fold change in fluorescence signal compared to tumor signals for each tissue type in mice treated with the indicated probes. (Student's T-test, Benforroni-Holm Procedure: **$p < 0.01$, ***$p < 0.001$). (**e**) Fluorescence microscopy images of 4T1 tumor sections from mice treated with the **AND-gate 2 probe** and stained for cleaved Casp3 and CD68 using specific antibodies. Single channel images are in grayscale. Merge images are as follows: Cy5 (probe) is magenta, CD68 is yellow, cleaved Casp3 is green, DAPI is blue. The same contrast and brightness settings were used to process each channel.

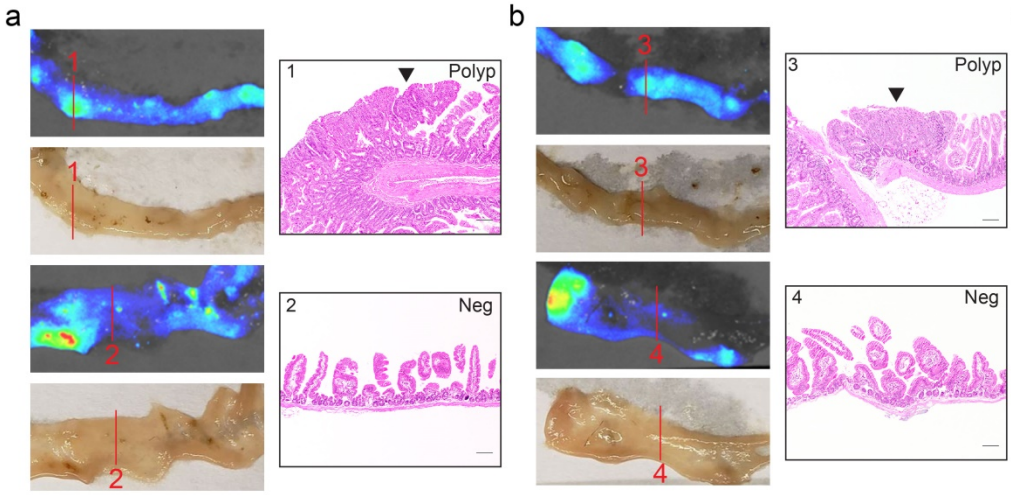

	6-QC	AND-Gate 2
TP	9	13
FP	4	2
TN	8	6
FN	3	3
FPR	0.33	0.25
FNR	0.25	0.19
Acc.	0.71	0.79

Figure 4. Imaging with the AND-Gate probe in a mouse model of colorectal cancer. Mice containing the $Apc^{min/+}$ allele were aged 22 weeks and injected with **6-QC** or **AND-Gate 2** (R.O., 20 nmol). The mice were sacrificed 16 h post injection and tissues were splayed open for fluorescent imaging. (**a-b**) Representative rainbow plot of fluorescent intensity and white light image of splayed colon tissue from mice injected with (**a**) **6-QC** or (**b**) **AND-Gate 2**. Tissue was sectioned at numbered positions, H&E stained, and evaluated for the presence of tumor (sections 1 and 3 are examples of true positives; 2 & 4 are examples of true negatives). All images were contrast adjusted to show the difference between signal within polyps and normal tissue. (**c**) Areas in splayed intestines with high, medium, or low fluorescence intensity were sectioned, H&E stained, and evaluated for the presence or absence of tumors. For **6-QC** and **AND-Gate 2**, 13 and 15 areas respectively of high fluorescent signal (expected to contain tumors), and 11 and 9 sections respectively were taken with low fluorescent signal (expected to be healthy tissue). Sections were binned into four categories: true positive (contained tumor as expected, TP), false positive (unexpected tumor, FP), true negative (expected healthy tissue, TN), and false negative (unexpected healthy tissue, FN). Based on the sectioning results the false-positive rate (FPR), false-negative rate (FNR), and accuracy for each probe was calculated (n = 3 mice per probe). Rainbow plots of all data used for analysis, can be found in the Supplemental Information (**Supplementary Figure 6 & 7**).